Japanese Journal of Applied Physics

Signal Characteristics of Super-Resolution Near-Field Structure Disk in Blue Laser System

Japanese Journal of Applied Physics
Vol. 43, No. 7B, 2004, pp. 4921–4924

Signal Characteristics of Super-Resolution Near-Field Structure Disk in Blue Laser System

Jooho KIM*, Inoh HWANG, Hyunki KIM, Duseop YOON, Insik PARK, Dongho SHIN,
Yunchang PARK[1] and Junji TOMINAGA[2]

Digital Media R&D Center, SAMSUNG ELECTRONICS CO., LTD, Suwon 442-742, Korea
[1]*Analytical Engineering Center, Samsung Advanced Institute of Technology, Kihung, Yongin 449-712, Korea*
[2]*Center for Applied Near-Field Optics Research, National Institute of Advanced Industrial Science and Technology (AIST), Tsukuba 305-8563, Japan*

(Received December 8, 2003; accepted February 17, 2004; published July 29, 2004)

We report the signal characteristics of a super-resolution near-field structure (super-RENS) disk in a blue laser system (laser wavelength, 405 nm; numerical aperture (NA), 0.85). By introducing a new structure for the blue laser system, a 42.5 dB carrier to noise ratio (CNR) at a 50-nm-mark-length-signal (which is equivalent to a 75 GB capacity with a 0.32 micrometer track pitch and a 1–7 modulation code (Blu-ray disc (BD) format)) and a much higher readout-stability were obtained. Transmission electron inicroscope (TEM) image analysis revealed that the new blue structure has clear diffusion protection barriers produced by continuous Pt particles, which is related to higher CNR and readout stability characteristics.
[DOI: 10.1143/JJAP.43.4921]

KEYWORDS: super-RENS, blue laser system, $ZnS\text{-}SiO_2$ inserted PtO_x, readout stability

1. Introduction

Together with a solid immersion lens (SIL),[1)] a multi level (layer) recording,[2,3)] a three-dimensional memory[4,5)] and a multi layer Blu-ray disc (BD),[6)] the super-resolution near-field structure (super-RENS) technology, which is one of the promising technologies for a sub-terabyte optical storage, has been progressed from an Sb mask type to a PtO_x mask type during the last 4 years.[7–11)] A huge signal enhancement up to above 40 dB carrier to noise ratio (CNR) for signals of marks shorter than 80 nm has already been achieved by a rigid elliptical bubble formation at a PtO_x layer sandwiched by AgInSbTe layers with the super-RENS technology in a 635 red laser system.[12)] The recording mechanism was proven to be the rigid elliptical bubble formation at the PtO_x layer by TEM cross-sectional image observation. The readout mechanism of a super-RENS disk is not clear at the moment, although Pt nano particle surface plasmon resonance (SPR) amplification and optical property changes of GeSbTe, PtO_x, $ZnS\text{-}SiO_2$ layers by thermal activation have been proposed.[12–15)] The super-RENS disk has several important issues such as readout stability, random signal jitter and error rate. These characteristics must be improved to commercialize the super-RENS sub-terabyte optical storage system. In this work, together with the CNR improvement of a 50-nm-mark-length signal, we attempted to make the readout stability higher.

2. Experimental Procedure

Sample disks were prepared using a magnetron sputtering method on a 1.1 mm polycarbonate substrate followed by a 0.1 mm cover layer coating. To examine recording and readout characteristics, an optical disk drive tester (a Pulstec DDU-1000, a laser wavelength (λ), 405 nm; lens numerical aperture (NA), 0.85) was used. The sample disks were rotated at a constant linear velocity of 5.0 m/s and the resolution bandwidth (RBW) of the signal spectrum analyzer was 30 kHz. The cross sections of the disks were also observed to investigate the disk structure and the deterioration mechanism of readout stability using a transmission electron microscope (TEM). Thermo-optical properties and optical constants were estimated using an ellipsometer (Mizojiri Optical Co., DHA-OLX/S4M) and a multi channel photo detector (Hamamatsu Photonics, PMA-11). The composition of the PtO_x layer was estimated by Rutherford back-scattering spectrometry (RBS) and nuclear reaction analysis (NRA).

3. Results and Discussion

The sample structure for a conventional red laser system[12)] and the new sample layer structure for the blue laser system are depicted in Figs. 1(a) and 1(b). The new blue laser system structure has a $ZnS\text{-}SiO_2$-inserted PtO_x (ZIP) layer. In the red structure, the reaction interface for writing is at the upper and lower interfaces of the PtO_x layer as shown in Fig. 1(c), which results in an unclear interface between the PtO_x and upper and lower $ZnS\text{-}SiO_2$ layers. In the case of using the ZIP layer, the reaction interface is inside of the PtO_x layer (Fig. 1(d)). From this result, it is thought that the writing reaction starts at the interface between the $ZnS\text{-}SiO_2$ and PtO_x layers. TEM image analysis also shows that the new blue structure has clear marks produced by continuous Pt particles, which is related to a higher CNR. By the thermo-optical property measurement, Rutherford RBS and nuclear reaction analysis (NRA), the decomposition temperature of PtO_x for writing is determined to be approximately 550°C[12,16)] and the composition of PtO_x is $PtO_{1.1}$.

Figure 2(a) shows the track direction cross-sectional TEM image of the sample disk showing the bubble. During the bubble formation process, GeSbTe phase change layers, particularly upper GeSbTe layer, are also deformed by the pressure of bubble formation. We can see that the upper $ZnS\text{-}SIO_2$ layer is also partially damaged by the bubble formation writing power. The size of Pt nano-particles is around below 5 nm as shown in Fig. 2(a). The atom arrangement inside the bubble is shown in Fig. 2(b). A partially textured atom array is detected and the unknown white area of the bubbles in Fig. 2(a) is uniformly filled with atoms. These atoms play an important role in super-

*E-mail address: jooho1.kim@samsung.com

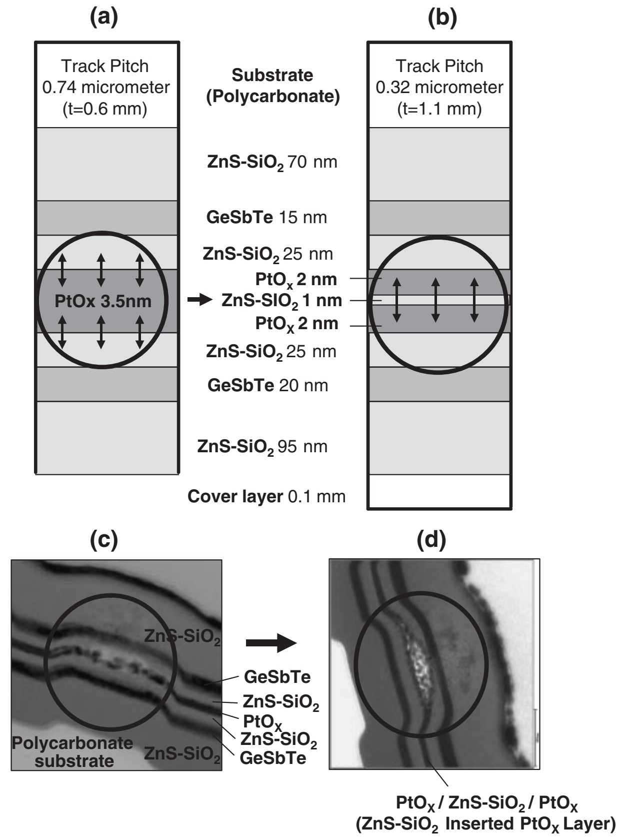

Fig. 1. Sample structure and radial direction TEM images: (a) conventional structure with PtO_x single layer, (b) new structure with $ZnS\text{-}SiO_2$-inserted PtO_x layer, (c) unclear 75 nm mark shape of conventional structure and (d) clear 75 nm mark shape of blue structure.

resolution phenomena in the super-RENS disk.

The frequency response characteristics of the sample disks are depicted in Fig. 3(a). The 405-nm-laser-wavelength (NA, 0.85) optical system is used for the signal characteristic measurement (resolution limit, 120 nm). The CNRs of the 300-nm-, 150-nm-, 75-nm- and 50-nm-mark-length signals are 55 dB, 51.5 dB, 45 dB and 42.5 dB, respectively. The 50 nm mark length used as a minimum mark length with a 0.32 micrometer track pitch is equivalent to a 75 GB capacity. Figure 3(b) shows before- and after-equalization (using a conventional EQ for BD with an approximately 8 dB boosting factor) RF waveforms of the 75-nm-mark-length signal. A relatively clear and uniform waveform is obtained.

Another distinctive feature of the super-RENS is the threshold phenomenon of a readout signal. Figure 4(a) shows the readout threshold phenomenon of the 50-nm-mark-length signal. The CNRs at 1.1 mW and 1.3 mW were 0 dB and 36 dB, respectively. This implies that the 0.2 mW readout power change produces an energy intensity amplification of around 10^4. We found another threshold phenomenon at around 2.0 mW readout power. We think that these results would be surely related to the super-RENS readout mechanism. However, the mechanism is not clear at the moment, thus we need further work to elucidate it. Figure 4(b) reveals the CNR spectrum showing 42.5 dB at 50 MHz, which corresponds to the 50-nm-mark-length signal at 5 m/s constant linear velocity (CLV).

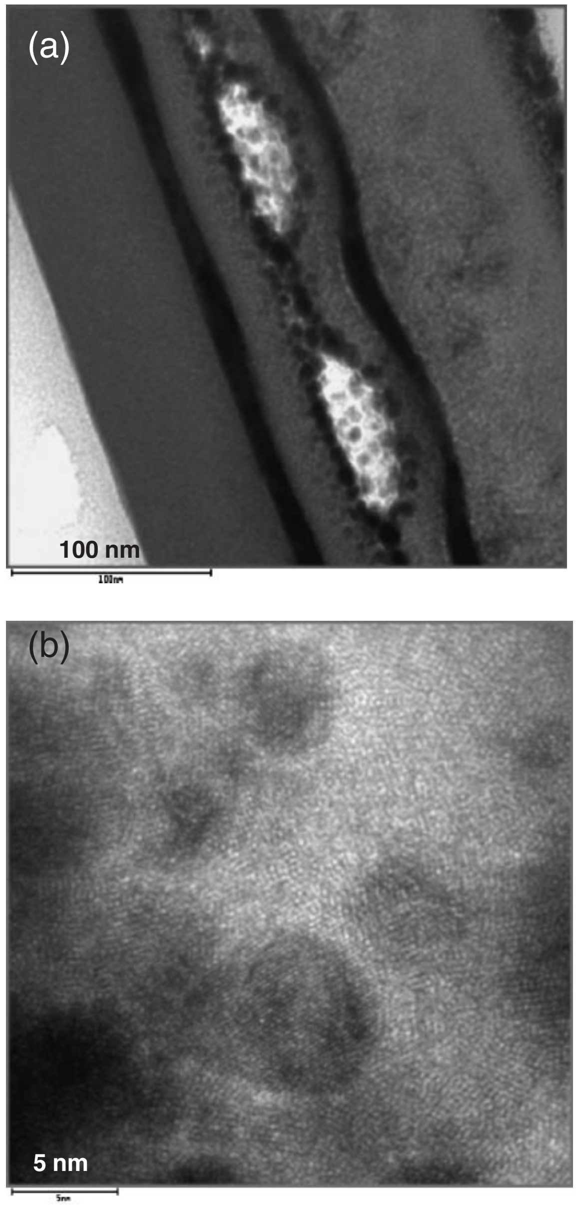

Fig. 2. Cross-sectional TEM images: (a) track direction cross-sectional TEM image showing bubble and (b) atom arrangement inside the bubbles.

The readout stability characteristics and the deterioration mechanism are depicted in Fig. 5. Up to 10^5 readout times, there is no signal deterioration in both 300-nm- and 75-nm-mark length signals as shown in Fig. 5(a). Figures 5(b) and 5(c) show initial state of CNR 43 dB and the deteriorated state of CNR 33 dB after 100 times of 3.5 mW reading, which is an acceleration condition for the stability test. From this result, deterioration is related to the damage of the upper GeSbTe phase change layer, caused by the diffusion of materials inside the bubble. As shown in Fig. 5(c), degradation occurs with different states at each bubble positions under the same readout power and times. It is thought that this non-uniformity might be related to the non-uniform state of the thin films of the sample disk. The conventional structure (Fig. 1(a)) must be more easily deteriorated by thermal activated diffusion. We think that the continuous Pt nano-particles of the new $ZnS\text{-}SiO_2$-inserted PtO_x (ZIP) structure play an important role as diffusion protection barriers to prevent material diffusion around the bubble.

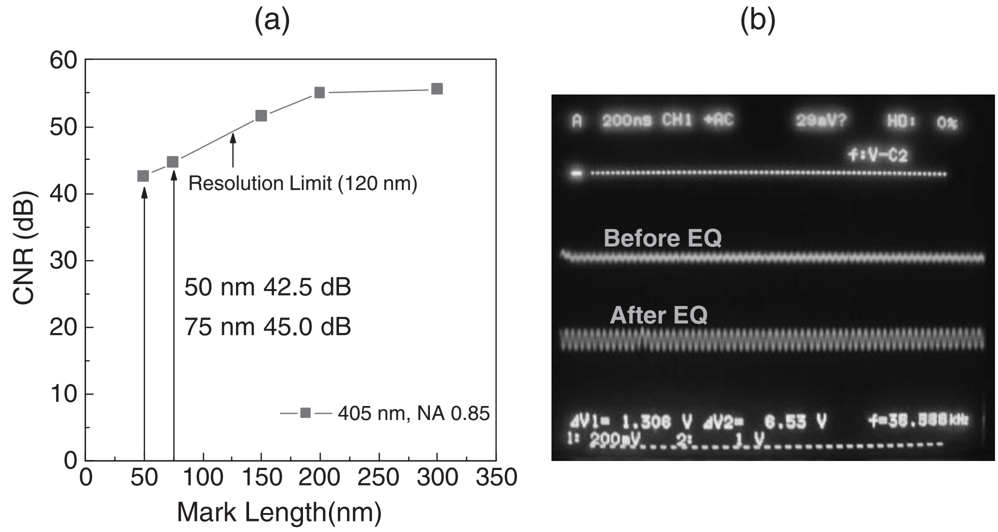

Fig. 3. Signal characteristics of the sample disks: (a) frequency response and (b) RF waveform of 75 nm mark signal.

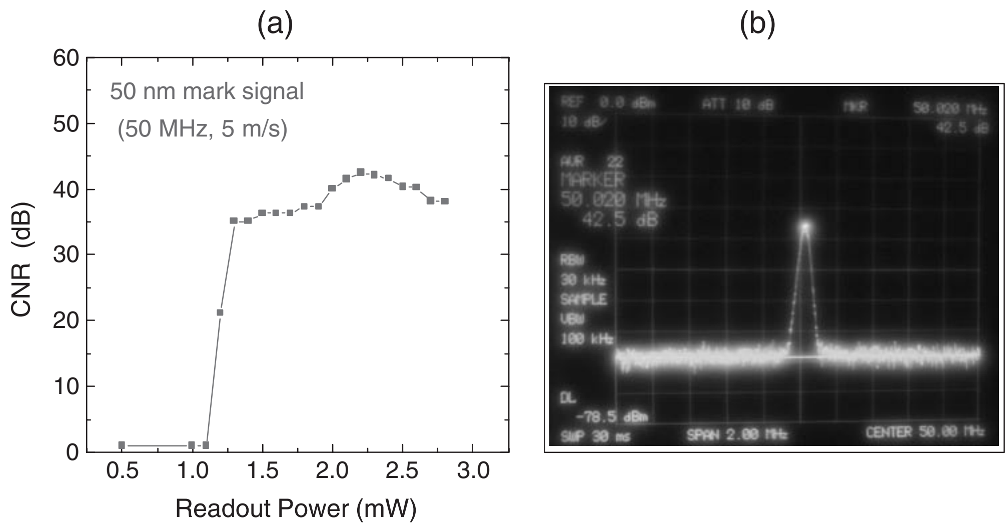

Fig. 4. Threshold characteristics and 50 nm CNR of the sample disk: (a) readout power dependence and (b) CNR spectrum showing 42.5 dB for 50 nm mark signal.

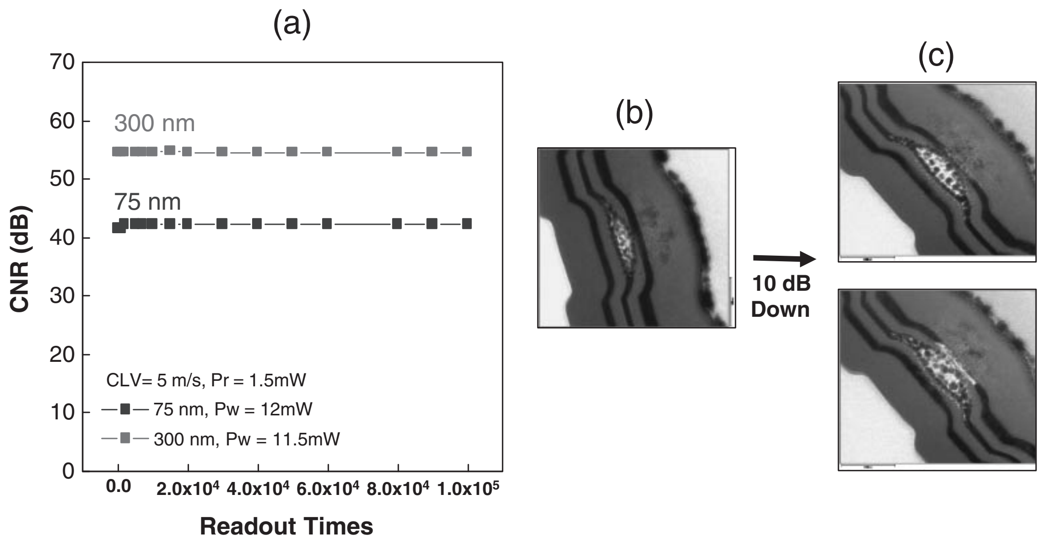

Fig. 5. Stability characteristics and deterioration mechanism: (a) readout stability, (b) initial state of CNR 43 dB and (c) deteriorated states of CNR 33 dB after 100 times of 3.5 mW reading.

4. Conclusion

We confirmed the super-RENS effect not only in the red laser system (wavelength, 635 nm; NA, 0.65) but also in the blue laser system (wavelength, 405 nm; NA, 0.85). The CNR of the 50 nm mark length signal was 42.5 dB by clear mark formation using a new ZnS-SiO_2-inserted PtO_x (ZIP) structure. The stability characteristic was also largely improved with the new designed structure. The result of this work indicates the possibility of a 75 GB capacity storage medium with a 0.32 micrometer track pitch.

1) F. Guo, T. Schlesinger and D. Stancil: Appl. Opt. **39** (2000) 324.
2) D. Day and M. Gu: Appl. Phys. Lett. **80** (2002) 2404.
3) K. Daly-Flynn and D. Strand: Jpn. J. Appl. Phys. **42** (2003) 795.
4) M. Irie, S. Kobatake and M. Horichi: Science **291** (2001) 1769.
5) S. Kawata and Y. Kawata: Chem. Rev. **100** (2000) 1777.
6) K. Mishima, H. Inoue, M. Aoshima, T. Komaki, H. Hirata and H. Utsunomiya: SPIE **5069** (2003) 90.
7) J. Tominaga, T. Nakano and N. Atoda: Appl. Phys. Lett. **73** (1998) 2078.
8) J.H. Kim, D. Buechel, T. Nakano, J. Tominaga, N. Atoda, H. Fuji and Y. Yamakawa: Appl. Phys. Lett. **77** (2000) 1774.
9) H. Fuji, J. Tominaga, L. Men, T. Nakano, H. Katayama and N. Atoda: Jpn. J. Appl. Phys. **39** (2000) 980.
10) J. H. Kim, M. Kuwahara, J. Tominaga and N. Atoda: Appl. Phys. Lett. **79** (2001) 2600.
11) J. H. Kim, I. Hwang, D. Yoon, I. Park, D. Shin, M. Kuwahara and J. Tominaga: Jpn. J. Appl. Phys. **42** (2003) 1014.
12) J. H. Kim, I. Hwang, D. Yoon, I. Park, D. Shin, T. Kikukawa, T. Shima and J. Tominaga: Appl. Phys. Lett. **83** (2003) 1701.
13) T. Kikukawa, T. Nakano, T. Shima and J. Tominaga: Appl. Phys. Lett. **81** (2002) 4697.
14) M. Ohtsu: *Small Particle of Light* (SHOKABO, Tokyo, 2001) p. 36 [in Japanese].
15) Y. R. Shen: *The Principles of Nonlinear Optics* (JOHN WILEY & SONS, New York, 1984) p. 541.
16) Y. Abe, M. Kawamura and K. Sasaki: Jpn. J. Appl. Phys. **38** (1999) 2092.